ELSEVIER

www.elsevier.nl/locate/ica

Inorganica Chimica Acta 304 (2000) 260–267

Inorganica Chimica Acta

Synthesis, structure and properties of molybdenum(VI) oxalate complexes of the types $M_2[Mo_2O_5(C_2O_4)_2(H_2O)_2]$ and $M_2[MoO_3(C_2O_4)]$ (M = Na, K, Rb, Cs)

Marina Cindrić [a,*], Neven Strukan [a], Višnja Vrdoljak [a], Maja Devčić [a], Zorica Veksli [b], Boris Kamenar [a]

[a] *Chemistry Department, Laboratory of General and Inorganic Chemistry, Faculty of Science, University of Zagreb, Ulica kralja Zvonimira 8, 10000 Zagreb, Croatia*

[b] *Rudjer Bošković Institute, POB 1016, 10000 Zagreb, Croatia*

Received 30 November 1999; accepted 2 February 2000

Abstract

The reaction of molybdenum(VI) oxide with oxalic acid or alkali oxalate and alkali halides results in the formation of two series of molybdenum(VI) oxalate complexes: one of the general formula $M_2[Mo_2O_5(C_2O_4)_2(H_2O)_2]$ containing the Mo_2O_5 core and the other of the formula $M_2[MoO_3(C_2O_4)]$ with a MoO_3 core (M = Na, K, Rb, Cs). Both series were characterized by chemical analysis, ESR, UV and IR spectroscopy, thermogravimetry, differential scanning calorimetry, X-ray powder method and some of them by single-crystal X-ray structure analysis. Complexes of the first series adopt dimeric structures, the second series infinite polymeric structures. In both types of structures molybdenum ions are six-coordinated being surrounded by terminal oxo-oxygens, bridging oxygens and bidentate bonded oxalate ligands. When exposed to UV light all these complexes in the solid state exhibit photochromic behavior changing color from colorless to green–brown. These changes are remarkably more pronounced in the complexes with dimeric structures. There is definite correlation between their coloration and the UV induced ESR signal indicative for molybdenum(V). Such behavior is explained by the partial reduction of Mo(VI) to Mo(V) only at the crystal surfaces. This is also the explanation why $K_2[Mo_2O_5(C_2O_4)_2(H_2O)_2]$ was so far described as being red or pale reddish tan. All attempts to prepare the corresponding lithium complexes were unsuccessful. They are most probably very unstable because of the small radius of the lithium ion.

Keywords: Crystal structures; Molybdenum complexes; Oxalato complexes; Dinuclear complexes

1. Introduction

Interest in the study of inorganic oxalates has resulted largely from use of oxalates in analytical chemistry and industry [1]. However, molybdenum(VI) oxalates are additionally interesting because of their solid state photochemistry and photochromism. Such behavior was first observed by Rosenheim [2] at the end of last century and later confirmed by Mentzen and Sauterean [3]. On being exposed to UV radiation Mo(VI) oxalate complexes change considerably from colorless to green or brown as the consequence of partial changes in the oxidation state of the metal. Molybdenum(VI) forms a variety of anionic oxomolybdenum oxalates and some of them have been known for many years [2–8] but only for a few, such as $K_2[Mo_2O_5(C_2O_4)_2(H_2O)_2]$ [4], $NaNH_4[MoO_3(C_2O_4)]\cdot 8H_2O$ [5], $[(-)Co(en)_3][MoO_3(C_2O_4)(H_2O)]\cdot 2H_2O$ [6] and $[(CH_3)_4N]_2[Mo_2O_5(C_2O_4)_2(H_2O)_2]$ [7], crystal structures have been determined by X-ray analysis. Also identified are complexes of the type $R_2[Mo_2O_5(C_2O_4)_2(H_2O)_2]$ (R = Rb, Cs, NH_4) [8], but their structures have been postulated only on the basis of spectral data. It seems that the structure type of these anionic complexes of molybdenum essentially depends upon the size of the cation and the pH of the solution from which they were crystallized.

* Corresponding author. Fax: +385-1-461 1191.
E-mail address: marina@chem.pmf.hr (M. Cindrić)

0020-1693/00/$ - see front matter
PII: S0020-1693(00)00098-0

In this paper we describe two series of Mo(VI) complexes; one of the type $M_2[Mo_2O_5(C_2O_4)_2(H_2O)_2]$ containing the Mo_2O_5 core and the other of the type $M_2[MoO_3(C_2O_4)]$ with the MoO_3 core. Alkali metals (M = Na, K, Rb, Cs) are the cations in both types of complexes. All compounds were characterized by chemical analysis, ESR, UV and IR spectroscopy, thermogravimetry, differential scanning calorimetry and X-ray powder diffraction diagrams. Some of them were also subjected to single-crystal X-ray structure analysis.

2. Experimental

2.1. Preparation of $M_2[Mo_2O_5(C_2O_4)_2(H_2O)_2]$ (1–4) and $M_2[MoO_3(C_2O_4)]\cdot xH_2O$ (5–8)

Complexes of the type $M_2[Mo_2O_5(C_2O_4)_2(H_2O)_2]$ (M = Na, K, Rb, Cs) (**1**–**4**) were prepared by mixing molybdenum(VI) oxide, oxalic acid dihydrate and corresponding alkali halides [10]. Complexes of the general formula $M_2[MoO_3(C_2O_4)]\cdot xH_2O$ (M = Na, $x = 3$; M = K, Rb, $x = 1$) (**5**–**7**) and $M_2[MoO_3(C_2O_4)]$ (M = Cs) (**8**) were also prepared from alkali oxalates and molybdenum(VI) oxide [3]. The crystals suitable for X-ray structure analyses were grown by slow evaporation of the aqueous solution obtained from the above described preparations. Molybdenum was determined according to the literature method [9] and oxalate by titration with potassium permanganate [10].

2.1.1. Complex **1**

Yield: 23%. *Anal.* Calc. for $C_4H_4Mo_2Na_2O_{15}$: $C_2O_4^{2-}$, 33.21; Mo, 36.21. Found: $C_2O_4^{2-}$, 32.91; Mo, 36.34%. IR (KBr) ν (cm^{-1}); 1675 $(CO_2)_{as}$, 1397 $(CO_2)_s$, 959 (MoO_t), 922 (MoO_t), 850 (Mo_2O_b), 804 (Mo_2O_b).

2.1.2. Complex **2**

Yield: 82%. *Anal.* Calc. for $C_4H_4K_2Mo_2O_{15}$: $C_2O_4^{2-}$, 31.31; Mo, 34.16. Found: $C_2O_4^{2-}$, 31.40; Mo, 34.12%. IR (KBr) ν (cm^{-1}); 1663 $(CO_2)_{as}$, 1393 $(CO_2)_s$, 961 (MoO_t), 920 (MoO_t), 848 (Mo_2O_b), 791 (Mo_2O_b).

2.1.3. Complex **3**

Yield: 76%. *Anal.* Calc. for $C_4H_4Mo_2O_{15}Rb_2$: $C_2O_4^{2-}$, 26.88; Mo, 29.29. Found: $C_2O_4^{2-}$, 26.81; Mo, 29.23%. IR (KBr) ν (cm^{-1}); 1672 $(CO_2)_{as}$, 1397 $(CO_2)_s$, 959 (MoO_t), 922 (MoO_t), 849 (Mo_2O_b), 802 (Mo_2O_b).

2.1.4. Complex **4**

Yield: 79%. *Anal.* Calc. for $C_4H_4Cs_2Mo_2O_{15}$: $C_2O_4^{2-}$, 23.48; Mo, 25.59. Found: $C_2O_4^{2-}$, 23.51; Mo, 25.60%. IR (KBr) ν (cm^{-1}); 1682 $(CO_2)_{as}$, 1404 $(CO_2)_s$, 949 (MoO_t), 904 (MoO_t), 795 (Mo_2O_b).

2.1.5. Complex **5**

Yield: 23%. *Anal.* Calc. for $C_2H_6MoNa_2O_{10}$: $C_2O_4^{2-}$, 26.51; Mo, 28.91. Found: $C_2O_4^{2-}$, 26.76; Mo, 29.20%. IR (KBr) ν (cm^{-1}); 1680 $(CO_2)_{as}$, 1440 $(CO_2)_s$, 920 (MoO_t), 872 (MoO_t), 743 (Mo_2O_b).

2.1.6. Complex **6**

Yield: 50%. *Anal.* Calc. for $C_2H_2K_2MoO_8$: $C_2O_4^{2-}$, 26.82; Mo, 29.23. Found: $C_2O_4^{2-}$, 26.76; Mo, 29.20%. IR (KBr) ν (cm^{-1}); 1680 $(CO_2)_{as}$, 1440 $(CO_2)_s$, 915 (MoO_t), 876 (MoO_t), 744 (Mo_2O_b).

2.1.7. Complex **7**

Yield: 48%. *Anal.* Calc. for $C_2H_2MoO_8Rb_2$: $C_2O_4^{2-}$, 20.91; Mo, 22.79. Found: $C_2O_4^{2-}$, 21.00; Mo, 22.82%. IR (KBr) ν (cm^{-1}); 1664 $(CO_2)_{as}$, 1439 $(CO_2)_s$, 912 (MoO_t), 874 (MoO_t), 748 (Mo_2O_b).

2.1.8. Complex **8**

Yield: 35%. *Anal.* Calc. for $C_2H_2Cs_2MoO_7$: $C_2O_4^{2-}$, 17.68; Mo, 19.27%. Found: $C_2O_4^{2-}$, 17.61; Mo, 19.30%. IR (KBr) ν (cm^{-1}); 1681 $(CO_2)_{as}$, 1432 $(CO_2)_s$, 897 (MoO_t), 869 (MoO_t), 751 (Mo_2O_b).

2.2. ESR spectra

ESR spectra were measured at 293 K using a Varian E-109 spectrometer operating at 100 kHz modulation, equipped with dual sample cavity. As a g-factor standard 2,2-diphenyl-1-picrylhydrazyl (DPPH, $g = 2.0036$) was used. When the complexes $M_2[Mo_2O_5(C_2O_4)_2(H_2O)_2]$ were exposed to UV light they changed from colorless to dark green and exhibited an ESR signal. The spectrum is characteristic for Mo(V) [11]. Paramagnetic (Mo^{5+}) concentration was determined by double integration of the spectrum and compared with the standard Varian strong pitch [12]. All compounds were exposed to UV light 10, 15, 30, 60 and 300 min.

The oxidation number of the molybdenum was also determined by titration with cerium(IV) sulfate (0.1 M, $f = 0.69850$, $V = 0.15$ cm^3) [13].

2.3. UV spectra

A Hewlett–Packard 8542A spectrophotometer was used in the range 100–350 nm. All solution spectra were measured in silica cells. The concentration of solutions used for measurement for compounds **2** and **6** were 2.59×10^{-5} mol dm^{-3} ($\varepsilon = 22442$ m^2 mol^{-1}) and 5.99×10^{-5} mol dm^{-3} ($\varepsilon = 8003$ m^2 mol^{-1}), respectively. Before measurements both complexes were exposed to UV light.

2.4. TG and DSC measurements

The complexes were also examined using thermogravimetry (TG) and differential scanning calorimetry (DSC). All thermal decompositions were recorded at a heating rate of 10°C min^{-1} in a dynamic atmosphere with a flow rate of 200 cm^3 min^{-1}. Aluminum crucibles were used under an argon or oxygen atmosphere. For all experiments the temperature range was 30–600°C. A Mettler TG 50 thermobalance was used to obtain thermogravimetric data. Calorimetric measurements were undertaken on a Mettler DSC 30 instrument. The results were developed by applying the GrafVare 2.1. program.

2.5. X-ray diffraction on powder

X-ray diffraction powder data were obtained using Cu Kα radiation ($\lambda = 1.5406$ Å) on a Philips PW 3710 diffractometer. Data were collected in the $3 < 2\theta < 65°$ range, in the θ–2θ step scan mode with $\Delta 2\theta = 0.02°$ and $t = 12$ s.

2.6. Single-crystal X-ray structure analysis

All data were collected on a Philips PW1100 diffractometer with graphite monochromatized Mo Kα radiation ($\lambda = 0.7107$ Å). The structures were solved by the heavy atom method and refined on F^2 by full-matrix least-squares calculations. Intensity data were corrected for absorption. All computations were performed on an IBM ThinkPad microcomputer (Pentium II 300 MHz) using SHELXS-97 [14] and SHELXL-97 [15]. The molecular and crystal structures drawings were prepared by ORTEP [16] and PLUTON [17].

2.7. Crystal data for complexes 3, 4, 6 and 7

$C_4H_4Mo_2O_{15}Rb_2$ (**3**), monoclinic, space group $P2_1/a$, $M_r = 654.90$, $a = 6.7902(7)$, $b = 14.3626(14)$, $c = 7.6228(7)$ Å, $\beta = 94.213(10)°$, $V = 741.40(10)$ $Å^3$, $Z = 2$, $D_x = 2.93$ g cm^{-3}, $F(000) = 612$, μ(Mo Kα) = 8.291 mm^{-1}. A single crystal of dimensions $0.30 \times 0.40 \times 0.30$ mm was used for data collection. Cell dimensions were determined using fitting angles for 30 strong reflections in the range $19 < 2\theta < 36°$. The 2141 unique reflections were collected by the ω–θ scan technique ($6 < 2\theta < 60°$, $-9 < h < 9$, $0 < k < 20$, $0 < l < 10$) at room temperature (r.t.). The calculations converged at $R(F) = 0.0484$ for 1788 reflections with $I \geq 2\sigma(I)$ and 108 refined parameters, $wR(F^2) = 0.1264$ for all data. The largest remaining difference peak was 2.19 e $Å^{-3}$ at 1.00 Å from Mo(1).

$C_4H_4Cs_2Mo_2O_{15}$ (**4**), monoclinic, space group $P2_1/a$, $M_r = 749.77$, $a = 6.0358(7)$, $b = 33.547(10)$, $c = 7.4996(10)$ Å, $\beta = 99.700(11)°$, $V = 1496.8(5)$ $Å^3$, $Z = 4$, $D_x = 3.33$ g cm^{-3}, $F(000) = 1368$, μ(Mo Kα) = 6.546 mm^{-1}. A single crystal of dimensions $0.30 \times 0.30 \times 0.20$ mm was used for data collection. Cell dimensions were determined using fitting angles for 21 strong reflections in the range $20.6 < 2\theta < 31.6°$. The 3229 unique reflections were collected by the ω–2θ scan technique ($5 < 2\theta < 54°$, $-7 < h < 7$, $0 < k < 42$, $0 < l < 9$) at r.t. The calculations converged at $R(F) = 0.0700$ for 2733 reflections with $I \geq 2\theta(I)$ and 209 refined parameters, $wR(F^2) = 0.2096$ for all data. The largest remaining difference peak was 2.47 e $Å^{-3}$ at 1.17 Å from Cs(1).

$C_2H_2K_2MoO_8$ (**6**), monoclinic, space group $P2_1/a$, $M_r = 328.18$, $a = 7.556(2)$, $b = 12.756(5)$, $c = 8.7050(10)$ Å, $\beta = 95.120(10)°$, $V = 835.7(4)$ $Å^3$, $Z = 4$, $D_x = 2.61$ g cm^{-3}, $F(000) = 632$, μ(Mo Kα) = 2.577 mm^{-1}. A single crystal of dimensions $0.25 \times 0.30 \times 0.25$ mm was used for data collection. Cell dimensions were determined using fitting angles for 21 strong reflections in the range $14 < 2\theta < 36.6°$. The 2434 unique reflections were collected by the ω–2θ scan technique ($5 < 2\theta < 60°$, $-10 < h < 10$, $0 < k < 17$, $0 < l < 12$) at r.t. The calculations converged at $R(F) = 0.0424$ for a 2315 reflections with $I \geq 2\theta(I)$ and 126 refined parameters, $wR(F^2) = 0.1083$ for all data. The largest remaining difference peak was 2.39 e $Å^{-3}$ at 0.79 Å from Mo(1).

$C_2H_2MoO_8Rb_2$ (**7**), monoclinic, space group $P2_1/a$, $M_r = 420.92$, $a = 7.6465(15)$, $b = 13.261(3)$, $c = 8.9647(17)$ Å, $\beta = 96.148\ (18)°$, $V = 903.8(3)$ $Å^3$, $Z = 4$, $D_x = 3.09$ g cm^{-3}, $F(000) = 776$, μ(Mo Kα) = 12.164 mm^{-1}. A single crystal of dimensions $0.20 \times 0.30 \times 0.35$ mm was used for data collection. Cell dimensions were determined using fitting angles for 30 strong reflections in the range $17 < 2\theta < 38°$. The 2629 unique reflections were collected by the ω scan technique ($6 < 2\theta < 60°$, $-10 < h < 10$, $0 < k < 18$, $0 < l < 12$) at r.t. The calculations converged at $R(F) = 0.0750$ for 1963 reflections with $I \geq 2\theta(I)$ and 119 refined parameters, $wR(F^2) = 0.2234$ for all data. The largest remaining difference peak was 2.46 e $Å^{-3}$ at 0.78 Å from Mo(1).

3. Results and discussion

3.1. Photochromic behavior and ESR spectra

The photochromic behavior of many oxo-compounds of molybdenum have been interpreted on the basis of electron trapping within defects in their crystals [18–20]. Luminescence, another well known property of molybdates, is explained by the presence of luminescent centres based on a tetrahedral molybdate groups [21]. However, the same phenomenon has also been observed in $K_2[MoO_3(C_2O_4)]\cdot H_2O$, which contains octahedral MoO_6 groups [21].

All molybdenum(VI) oxalate complexes of the general formula $M_2[Mo_2O_5(C_2O_4)_2(H_2O)_2]$ with M = Na, K, Rb and Cs are colorless but when exposed to UV radiation their color changes to green–brown. However, contrary to such observations the potassium salt has also been described as being red or pale reddish tan [4]. Stimulated by this discrepancy as well as by the discussion concerning the distances and angles within this complex molecule [22–24], we decided to redetermine its crystal structure. Our structural finding is however essentially the same as that described by Cotton and co-workers [4].

All these complexes in the solid state exhibit a considerable photochromic behavior and our experiments showed a definite correlation between their coloration and their UV induced ESR signal. When protected from UV light they do not show any signal but, once exposed, the signal was evident in all cases. The intensity of the ESR spectrum was not time-dependent because after 5 h exposure it remained unchanged. The concentration of paramagnetic Mo^{5+} induced by UV was about 10^{17} ions per gram, for all three powdered samples. However, the intensity of the spectra changed with the surface area of compounds. The single crystals exhibited very low paramagnetic Mo^{5+} concentration and spectra were difficult to integrate. The results obtained by the titration of the aqueous solutions of such partially reduced complexes with $Ce(SO_4)_2$ were in agreement with conclusion, since the observed oxidation numbers of molybdenum were about + 5.8. It was also noted that the IR spectra as well as the single-crystal diffraction patterns remained unchanged and were independent of the UV radiation. Such observations might lead to the conclusion that the partial reduction of Mo(VI) to Mo(V) occurs only at crystal surfaces.

However, when the oxalate complexes of the type $M_2[MoO_3(C_2O_4)]\cdot xH_2O$ (M = Na; $x = 3$; M = K, Rb; $x = 1$) and $M_2[MoO_3(C_2O_4)]$ (M = Cs) were exposed to UV the color change was not so evident being usually to a very pale pink, and nor were ESR signals observed. The polymeric nature of the complex anion and stabilization effect due to the interactions between oxalate ligands as well as between oxo-oxygen atoms are most probably the reason for such behaviour.

3.2. UV spectra

The UV spectra of aqueous solutions of UV-induced $M_2[Mo_2O_5(C_2O_4)_2(H_2O)_2]$ and $M_2[MoO_3(C_2O_4)]\cdot H_2O$ complexes showed the absorption maxima at 206 nm. According to the literature, these maxima can be interpreted as charge transfer bands [25–27]. In the UV region (30 000–50 000 cm^{-1}) the charge-transfer absorption spectra of most Mo(VI) polyoxoanions are attributed to the oxygen-to-metal transitions [28]. Upon irradiation, electrons are promoted from the low energy electronic states, mainly comprised of oxygen 2p orbitals, to the high-energy states, which are mainly comprised of metal d orbitals. The polyoxometalates contain two or three chromophores due to the bonding of the metal ion to the unshared (terminal) oxygens and to the edge and/or corner-shared oxygens. Since the bonding between a terminal oxygen and a metal ion possesses greater double bond character its charge-transfer transition usually appears in the high energy region ($> 40\ 000\ cm^{-1}$) [29–31]. The absorptions due to the other chromophores are seen in the lower energy region, e.g. M–O–M bridges are observed in the region between 30 000 and 40 000 cm^{-1}. An internal transition within the oxalate group should contribute to the absorbance above 35 000 cm^{-1} [25,32], but is likely to be weak and in 2 and 6 is not responsible for the peak at 48 543 cm^{-1}.

3.3. TG and DSC analyses

Our investigations of the thermal behavior of molybdenum(VI) complexes complete the results already known from the literature [33], and are in agreement with our crystal structure determinations.

The TG study reveals that two main endothermic processes occur: dehydration and pyrolitic decomposition (Table 1, Figs. 1 and 2). The dehydration of complexes with $Mo_2O_5^{2+}$ core (**1**–**4**) is accompanied by the decomposition of the oxalate without a stable intermediate product. However, in case of the complex **1**, the removal of water and decomposition of the oxalate groups proceed in a stepwise fashion. On the other hand, all anhydrous complexes with MoO_3 core (**5**–**8**) are stable in the particular temperature range beyond which the decomposition starts. Furthermore, complexes **1**–**4** start to release water molecules at higher temperature than complexes **5**–**8**. This suggests the presence of two differently bonded water molecules: coordinated water in the former and water of crystallization in the latter complexes. Both were proven to be present by the X-ray structure analyses. The thermal analysis curves suggest that the water molecules are more strongly bonded in the complexes when the cations are of smaller ionic radii, than in the complexes with larger radii. For instance, the crystals of $Cs_2[MoO_3(C_2O_4)]\cdot xH_2O$ lose water molecules at r.t. very easily so that their decomposition occurs rapidly. This is one reason why its crystal structure could not be determined; the other is that the crystal decomposition occurred during exposure to the X-rays. The weight loss for anhydrous complexes corresponds to the gradual loss of carbon monoxide and carbon dioxide and partial decomposition, most probably resulting in the formation of intermediate oxalate-carbonate compounds. As already known, the further loss of CO and CO_2 results in the formation of the end products [33]

Table 1
Thermoanalytical data for the complexes $M_2[Mo_2O_5(C_2O_4)_2(H_2O)_2]$ and $M_2[MoO_3(C_2O_4)]\cdot xH_2O$

Complex	DSC (°C)		TG (°C)		Mass loss (%) observed (calculated)
	Dehydration	Pyrolysis	Dehydration	Pyrolysis	
1	145	263 298	100–160	195–295 295–380	34.45 (33.93)
2	257		155–380		33.47 (32.04)
3	251		155–380		27.64 (27.50)
4	203		120–380		23.96 (24.02)
5	111 161	394	45–130 130–215	265–350 350–465	37.65 (37.99)
6	199	359	95–220	320–375 375–440	26.73 (27.14)
7	179	358	90–205	300–380 380–450	20.98 (21.39)
8		367	room temperature	290–405	20.98 (21.39)

$M_2Mo_2O_7$ (in the case of complexes with an $Mo_2O_5^{2+}$ core) and M_2MoO_4 (in the case of complexes with an MoO_3^{2+} core). From the DSC measurements it follows that the overall enthalpy change for the decomposition of **1**–**4** in argon atmosphere is about 20 kJ mol^{-1}, whereas the enthalpy for the dehydration of **5**–**8** amounts to approximately 53 kJ mol^{-1} and for the oxalate decomposition about 80–90 kJ mol^{-1}.

As previously observed during the decomposition of such complexes in an argon atmosphere, the molybdenum undergoes partial reduction from Mo(VI) to probably Mo(V) [1]. This thermal decomposition is followed by a sharp exothermic step in the temperature range 420–470°C and is related to the reoxidation of molybdenum on further heating. That process is accompanied by reduction of carbon monoxide to carbon, which is indicated by the black coloration of the residues. In order to obtain pure residues thermal decomposition was also undertaken in an atmosphere of pure oxygen. Data concerning the weight losses of the complexes are given in Table 1. Final solid products were characterized by powder X-ray diffraction and IR spectroscopy. The agreement between theoretical and experimental mass losses is within experimental error and is consis-

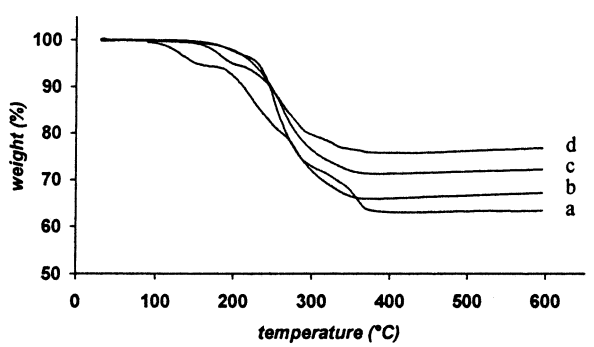

Fig. 1. TG curves for the thermal decomposition of complexes $M_2[Mo_2O_5(C_2O_4)_2(H_2O)_2]$ [M = Na (a), K (b), Rb (c), Cs (d)].

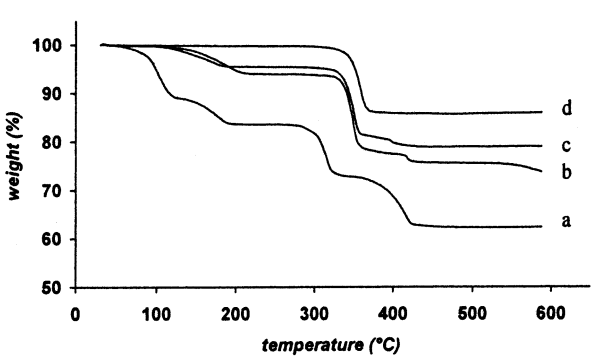

Fig. 2. TG curves for the thermal decomposition of complexes $M_2[MoO_3(C_2O_4)]\cdot xH_2O$ [M = Na (a), K (b), Rb (c), Cs (d)].

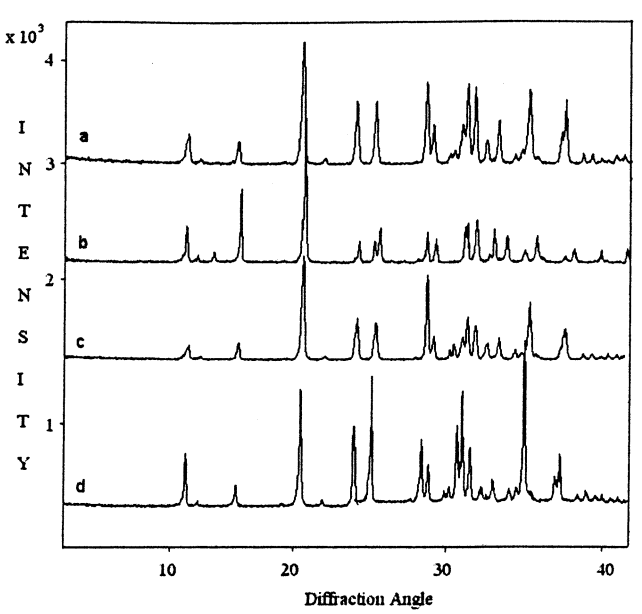

Fig. 3. Experimental XRD powder patterns for complexes $M_2[Mo_2O_5(C_2O_4)_2(H_2O)_2]$ [M = Na (a), K (b), Rb (c), Cs (d)].

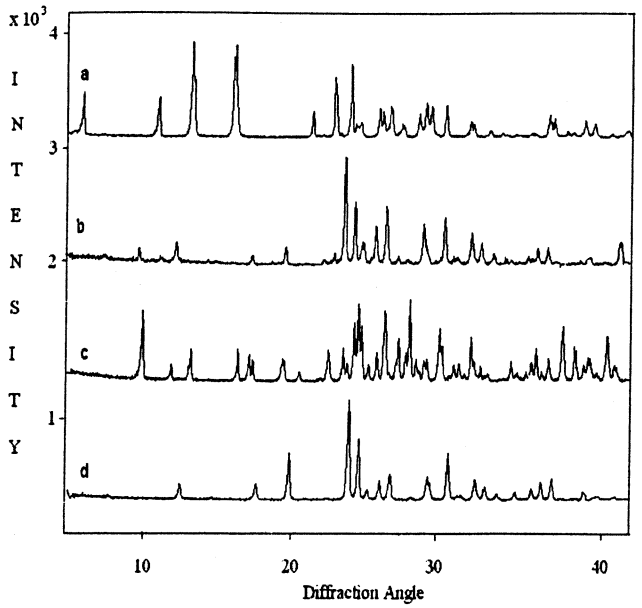

Fig. 4. Experimental XRD powder patterns for complexes $M_2[MoO_3(C_2O_4)]\cdot xH_2O$ [M = Na (a), K (b), Rb (c), Cs (d)].

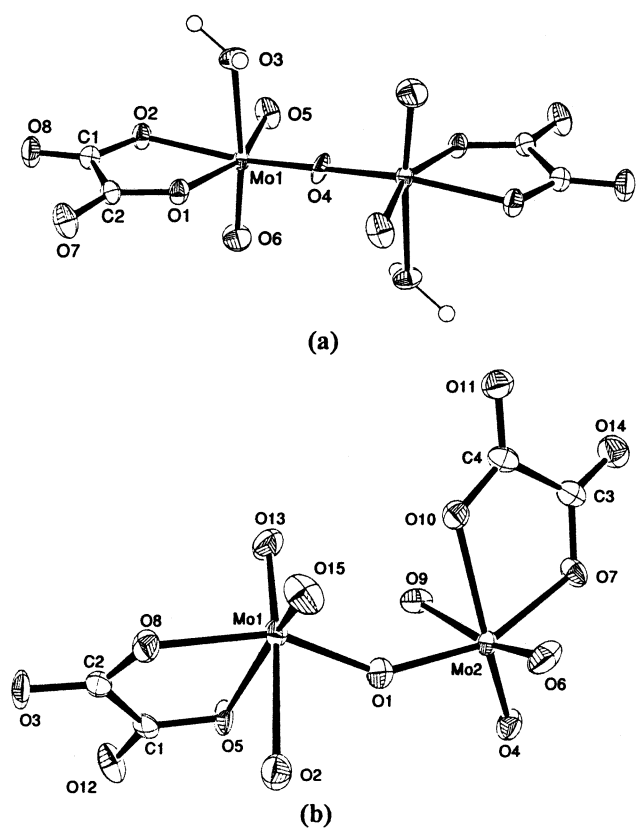

Fig. 5. Dimeric anion $[Mo_2O_5(C_2O_4)_2(H_2O)_2]^{2-}$ found in (a) potassium and rubidium salts; (b) caesium salt.

tent with the empirical formulation of each complex and the analytical data. The results are comparable with the analogous thermal studies already known from the literature [8,33–38]. The only disagreement is found for the thermal behavior of $Cs_2[MoO_3(C_2O_4)]\cdot xH_2O$ for which it has been claimed that the loss of water molecule started at 70°C [34].

3.4. Powder diffraction diagrams

The X-ray diffraction powder diagrams show great similarity within each class of complexes (Figs. 3 and 4). X-ray diffraction powder diagrams for $M_2[Mo_2O_5(C_2O_4)_2(H_2O)_2]$ complexes are similar, with the exception of the diagram of **4**, which is obviously not isostructural with **2** and **3** due to the size of cesium cation. Namely, the cation of larger ionic radii may induce distortion of the dimeric anion causing benting of the Mo–O–Mo bridge and therefore twisting of the oxalate ion planes. The powder patterns for $M_2[MoO_3(C_2O_4)]\cdot xH_2O$ are less similar, particularly at diffraction angles between $\theta = 10$ and 30°. The peaks are shifted towards larger diffraction angles indicating

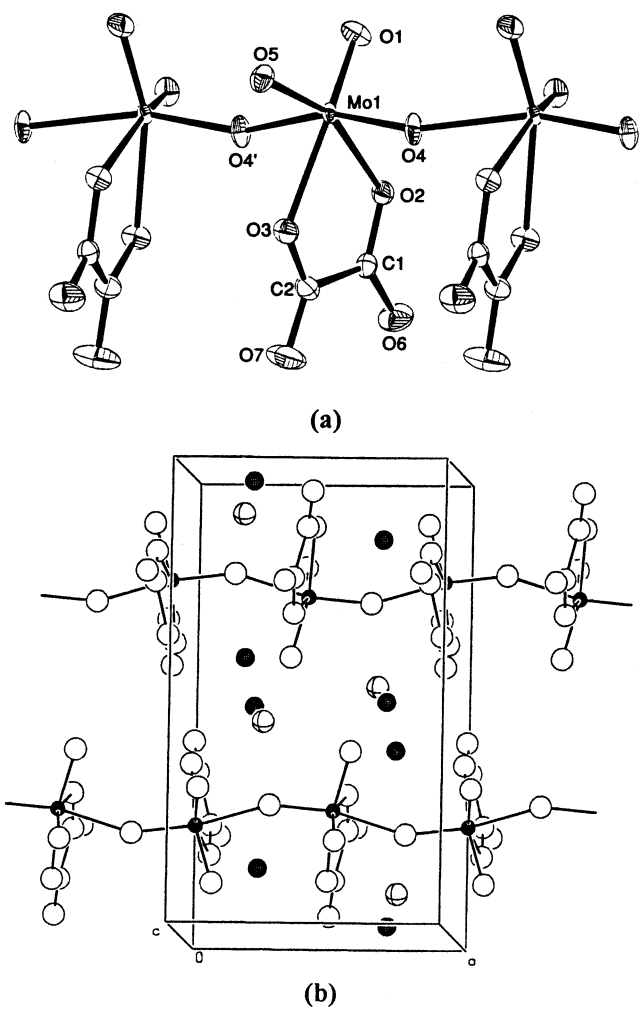

Fig. 6. (a) Polymeric $\{[MoO_3(C_2O_4)]^{2-}\}_n$ anion found in the structures of potassium and rubidium salts. (b) Unit cell packing diagram of isostructural potassium and rubidium salts. Shaded circles are K or Rb ions.

Table 2
Selected bond distances (Å) and angles (°) in oxalate complexes

Complex	Mo–O_t	Mo–O_b	Mo–OH_2	Mo–$O_{oxalate}$	Mo–O–Mo
$K_2[Mo_2O_5(C_2O_4)_2(H_2O)_2]$	1.680(19) [a]	1.876(2) [a]	2.3330(18) [a]	2.087(18) [a]	180 [a]
	1.700(20) [a]			2.186(18) [a]	
	1.693(2) [b]	1.8770(2) [b]	2.265(2) [b]	2.080(2) [b]	180 [b]
	1.705(2) [b]			2.184(2) [b]	
$Rb_2[Mo_2O_5(C_2O_4)_2(H_2O)_2]$	1.695(4)	1.8795(4)	2.279(4)	2.084(4)	180
	1.682(4)			2.167(4)	
$Cs_2[Mo_2O_5(C_2O_4)_2(H_2O)_2]$	1.703(8)			2.069(7)	
	1.693(8)	1.898(8)	2.372(8)	2.093(8)	
	1.710(8)	1.865(8)	2.357(8)	2.166(8)	144.7
	1.710(8)			2.159(8)	
$K_2[MoO_3(C_2O_4)]\cdot H_2O$	1.723(2)	1.784(2)		2.206(2)	151.73
	1.737(2)	2.136(2)		2.215(2)	
$Rb_2[MoO_3(C_2O_4)]\cdot H_2O$	1.729(7)	1.789(7)		2.202(6)	155.9
	1.735(6)	2.142(7)		2.206(7)	
$NaNH_4[MoO_3(C_2O_4)]\cdot 2H_2O$ [c]	1.815(4)	2.230(4)		2.235(4)	149.12
	1.850(4)	1.878(4)		2.242(4)	

[a] Ref. [4].
[b] Ref. [42].
[c] Ref. [5].

the expansion of the unit cell [39], e.g. for $K_2[MoO_3(C_2O_4)]\cdot H_2O$ $V = 835.70$ Å^3 and for $Rb_2[MoO_3(C_2O_4)]\cdot H_2O$ $V = 903.80$ Å^3. Obviously, the cation size also has effect on the polymeric structures. The end products of thermal decomposition of these two types complexes are different, as is confirmed by their X-ray powder diffraction patterns.

3.5. Single-crystal diffraction studies

The structures of the anions $[Mo_2O_5(C_2O_4)_2(H_2O)_2]^{2-}$ and of $\{[MoO_3(C_2O_4)]^{2-}\}_n$ resulting from single-crystal X-ray structure analyses are shown in Figs. 5 and 6, respectively. The most interesting interatomic distances are listed in Table 2. They are compared with the data found in the literature [4,5].

The dimeric anions found in the compounds $Rb_2[Mo_2O_5(C_2O_4)_2(H_2O)_2]$ (**3**) and $Cs_2[Mo_2O_5(C_2O_4)_2(H_2O)_2]$ (**4**) contain two octahedrally coordinated molybdenum(VI) ions sharing common corners at the bridging oxygen atoms. Whereas the bridge Mo–O–Mo in the anion of **3** is strictly linear due to the fact that the bridging oxygen atom occupies a center of symmetry, in the structure **4** this angle is 144.7(5)°. Consequently, the oxalate ion planes in **3** are parallel, in **4** they make an angle of 53.0(2)°. Both linear [8,40,41] and angular [4,7] structures are known in the crystal chemistry of molybdenum(VI) complexes. The first linear oxalato complex, $K_2[Mo_2O_5(C_2O_4)_2(H_2O)_2]$, was characterized by Cotton and co-workers [4]. A similar structure was also found in $(NH_4)_2[Mo_2O_5(C_2O_4)_2(H_2O)_2]$ [8,41].

The angles at the bridging oxygen can differ significantly, e.g. in the structure of $[(CH_3)_4N]_2[Mo_2O_5(C_2O_4)_2(H_2O)_2]$ [7] its value is 177(2)° so that the bonding is nearly linear. The six Mo–O bond lengths range from 1.682(4) to 2.279(4) Å in **3** and from 1.693(8) to 2.372(8) Å in **4**. They depend upon the bond order as well as upon the positions in the structure, i.e. *cis* or *trans* to the terminal or bridging oxo-oxygen atoms. Two Mo–OH_2 bonds are significantly longer amounting to 2.279(4) in **3** and 2.372(8) and 2.357(8) in **4**.

In the polymeric $\{[MoO_3(C_2O_4)]^{2-}\}_n$ anion found in $K_2[MoO_3(C_2O_4)]\cdot H_2O$ (**6**) and $Rb_2[MoO_3(C_2O_4)]\cdot H_2O$ (**7**) the molybdenum ions are also six-coordinated in the form of distorted octahedra being surrounded by two terminal oxo-oxygens, two bridging oxygens and two from the bidentate oxalate ligands. Both structures are bent with the Mo–O–Mo angle at 151.7(3)° in **6** and 155.9(4)° in **7**. The bridges are asymmetrical with the Mo(1)–O(4) bond lengths of 1.784(2) Å in **6** and 1.789(7) Å in **7** and with the Mo(1) –O(4′) bonds 2.136 (2) Å in **6** and 2.142 (7)Å in **7**. The two terminal Mo–O bond lengths are 1.723(2) and 1.737(2) Å in **6** and 1.729(7) Å and 1.735(6) Å in **7**. As far as we can ascertain, the only oxalate complex of Mo(VI) in which the polimeric $\{[MoO_3(C_2O_4)]^{2-}\}_n$ unit has been structurally characterized occurs in $NaNH_4[MoO_3(C_2O_4)]\cdot 8H_2O$ [5]. However, there is doubt about the accuracy of the determination because Atovmyan an Bokii reported unusual Mo–O_t bond lengths of 1.815(4) and 1.850(4) Å, so that any comparison with it is inappropriate. Namely, Spivack and Dori already criticized the result offered by the Russian authors [40].

All our attempts to prepare lithium complexes with either the Mo_2O_5 or the MoO_3 core were unsuccessful.

However, in experimenting with the aqueous solutions containing Li^+ and $[Mo_2O_5(C_2O_4)_2(H_2O)_2]^{2-}$ ions we noticed their extreme sensitivity to light. They rapidly undergo a color change from colorless to blue.

4. Supplementary material

Atomic coordinates, anisotropic displacement parameters, and bond distances and angles have been deposited with the Cambridge Crystallographic Data Centre: CCDC 132276 for compound **3**, CCDC 132277 for compound **4**, CCDC 132278 for compound **6** and CCDC 132279 for compound **7**. Copies of this information may be obtained free of charge from The Director, CCDC, 12 Union Road, Cambridge CB2 1EZ, UK (fax: +44-1223-336033; e-mail: deposit@ccdc.cam.ac.uk or www: http://www.ccdc.ac.uk).

Acknowledgements

Financial support for this research was provided by the Ministry of Science and Technology of the Republic of Croatia (Grant no. 119407).

References

[1] M.I. Diaz-Guemes, A.S. Bhatti, D. Dollimore, Thermochim. Acta 106 (1986) 125.
[2] A. Rosenheim, Z. Anorg. Chem. 4 (1893) 360.
[3] B.F. Mentzen, H. Sauterean, J. Photochem. 15 (1981) 169.
[4] F.A Cotton, S.M. Morehouse, J.S. Wood, Inorg. Chem. 3 (1964) 1603.
[5] L.O. Atovmyan, G.B. Bokii, J. Struct. Chem. 4 (1963) 524.
[6] L.R. Nassimbeni, M.L. Niven, J.J. Cruywagen, J.B.B. Heyns, J. Crystallogr. Spectrosc. Res. 17 (1987) 99.
[7] M. Cindrić, N. Strukan, V. Vrdoljak, Croat. Chem. Acta 72 (1999) 501.
[8] H.J. Becher, N. Amsoneit, U. Prigge, G. Gatz, Z. Anorg. Allg. Chem. 430 (1977) 255.
[9] G.A. Parker, Analytical Chemistry of Molybdenum, Springer-Verlag, New York, 1983.
[10] A.L. Vogel, Quantitative Inorganic Analysis, 3rd ed., Longmans Green, London, 1948, p. 338.
[11] M. Cindrić, D. Matković-Čalogović, B. Kamenar, Inorg. Chim. Acta 248 (1996) 103.
[12] D. Ćukman, J. Jednačak-Bišćan, Z. Veksli, W. Haller, J. Colloid Interface Sci. 111 (1987) 357.
[13] J.J. Stark, J. Chem. Educ. 64 (1969) 505.
[14] G.M. Sheldrick, SHELXS-96, Program for the solution of crystal structures, University of Göttingen, Germany, 1996.
[15] G.M. Sheldrick, SHELXL-96, Program for the refinement of crystal structures, University of Göttingen, Germany, 1996.
[16] C.K. Johnson, ORTEP-II, Rep. ORNL-5138, Oak Ridge National Laboratory, Oak Ridge, TN, 1976.
[17] A.L. Spek, in: D. Sayre (Ed.), Computational Crystallography, Clarendon Press, Oxford, 1982, p. 528.
[18] T. Yamase, T. Ikawa, H. Kokado, Chem. Lett. (1973) 617.
[19] T. Yamase, H. Hayashi, T. Ikawa, Chem. Lett. (1974) 1055.
[20] T. Yamase, J. Chem. Soc., Dalton Trans. (1978) 283.
[21] G. Blasse, G.J. Dirksen, J. Chem. Phys. Lett. 78 (1981) 234.
[22] J. Donahue, Inorg. Chem. 4 (1965) 921.
[23] F.A. Cotton, S.M. Morehouse, J.S. Wood, Inorg. Chem. 4 (1965).
[24] F.A. Cotton, R.M. Wing, Inorg. Chem. 4 (1965) 870.
[25] T. Yamase, Chem. Rev. 98 (1998) 307.
[26] J. Sobczak, J.J. Ziolkowski, J. Less-Common. Met. 54 (1977) 149.
[27] T. Yamase, R. Sasaki, T. Ikawa, J. Chem. Soc., Dalton Trans. (1981) 628.
[28] X.M. Zhang, B.Z. Shan, X.Z. You, Polyhedron 16 (1997) 95–102.
[29] K. Nomiya, Y. Sugie, K. Animato, M. Miwa, Polyhedron 6 (1987) 519–524.
[30] R. Neier, C. Trojanowski, R. Mattes, J. Chem. Soc., Dalton Trans. (1995) 2521.
[31] B. Kraut, G. Ferraudi, J. Chem. Soc., Dalton Trans. (1991) 2063.
[32] D.P. Graddon, J. Inorg. Nucl. Chem. 3 (1956) 308.
[33] J. Gopalakrishan, B. Viswanathan, V. Srinivasan, J. Inorg. Nucl. Chem. 32 (1970) 2565.
[34] S.P. Goel, P.N. Mehrotra, Thermochim. Acta 76 (1984) 127.
[35] S.P. Goel, P.N. Mehrotra, J. Less-Common Met. 106 (1985) 27.
[36] S.P. Goel, P.N. Mehrotra, Thermochim. Acta 95 (1985) 295.
[37] S.P. Goel, P.N. Mehrotra, Indian J. of Chem. A 24 (1985) 199.
[38] S.P. Goel, P.N. Mehrotra, Thermochim. Acta 70 (1983) 201.
[39] J.A. Wang, A. Morales, X. Bokhimi, O. Novaro, Chem. Mater. 11 (1999) 308–313.
[40] B. Spivack, Z. Dori, Coord. Chem. Rev. 17 (1975) 99–136.
[41] M. Cindrić, N. Strukan, V. Vrdoljak, M. Devčić, B. Kamenar, Inorg. Chim. Acta, in press.
[42] M. Cindrić, M. Devčić, N. Strukan, Molybdenum(VI) oxalato complexes, Seventh Slovenian-Croatian Crystallographic Meeting, Radenci, Slovenia, 1998, Abstracts p. 44.